

Characterization of Released Particles on the Surface of a Weathered Nanosilica/Polyurethane Coatings after Abrasion

Hsiang-Chun Hsueh^{1,2}, Chen-Yuan Lu^{1,3}, Sin-Ru Huang³, Yu-Lun Cheng³, Deborah Jacobs¹, Savelas A. Rabb¹, Lee L. Yu¹, Tinh Nguyen¹ and Lipiin Sung¹

¹National Institute of Standards and Technology, 100 Bureau Dr, Gaithersburg, MD 20899, USA

²National Tsing Hua University, No. 101, Section 2, Kuang-Fu Rd., Hsinchu 30013, Taiwan

³National Cheng Kung University, No.1, University Rd., Taiwan 701, Taiwan

ABSTRACT

Objective of this study is to understand the mechanism and process of nanoparticle release from nanocoatings under different environment stresses. A commercial PU coating having 5 % mass fraction of nanosilica was selected. Specimens were exposed in a well-controlled high-intensity UV environment at 50 °C and approximately 0 % relative humidity. After UV exposure, a mechanical abrasion test method was applied to induce particles release from UV exposed nanocoatings. Laser scanning confocal microscopy (LSCM) and atomic force microscopy (AFM) were used to characterize the surface morphological changes and nanoparticle accumulation on the coating surface at different exposure times. After abrasion, the number and size distribution of released particles on the abraded surfaces were also quantified using LSCM with image analysis. The effect of UV exposure time on the surface mechanical properties under abrasion will be examined and mechanical-induced particle release (through Si mass) will be quantified using inductively coupled plasma-optical emission spectroscopy (ICP-OES) and compared to the release results via simulated rain method from the same coating system.

Keywords: AFM, LSCM, nanocoating, particle release, ICP-OES, UV degradation, weathering

1 INTRODUCTION

Due to enhancement in performance properties such as increase in mechanical strength, thermal, chemical and ultraviolet (UV) resistance, nanoparticles have been incorporated into protective coatings used on building exterior, automotive, aerospace, and many outdoor applications.¹⁻⁴ When these protective nanocoatings are used in the outdoor settings, they will be exposed to mechanical and thermal stresses (e.g. abrasion and temperature extremes) and weathering (e.g., moisture [rain, snow], UV radiation). Nanoparticles may migrate to the coating surface then into environment under these stresses and these released particles may have adverse effects on the environment and human health.⁵⁻⁷

Many researches have attempted to understand the mechanism and the process of nanoparticle release under different environmental stresses.⁷⁻¹¹ Most researches focused on analyzing the contribution of individual stressor, there are little work on investigate the combination of many stressors in a practical setting. In our previous study,⁸ we have investigated the mechanism and process of nanosilica release of a commercial nanosilica/polyurethane coating using a simulated rain protocol on the UV-exposed nanocoatings. This study is a continuous effort to understand the mechanism of the particle release under combination of different environmental stressors. In this study, the same nanosilica/polyurethane coating system is used. Instead of using simulated rain to induce particle release from UV-exposed surface, a mechanical stressor is applied using a rotary abrader. Laser scanning confocal microscopy (LSCM) and atomic force microscopy (AFM) were used to characterize the nanosilica on the UV-exposed surface at different exposure times. A mechanical abrasion test method was applied to induce particles release from UV exposed surfaces. A combination of high resolution LSCM and image analyses were implemented to quantify the number and size distribution of released particles on the abraded surfaces. Finally, inductively coupled plasma-optical emission spectroscopy (ICP-OES) were used to analyze the Si mass assuming from release nanosilica collected from abraded surface and abrasion wheels. The results (release Si mass) from this method will be compared to the results from the simulated rain method at different UV exposure times from previous study.⁸

2 EXPERIMENTAL[◇]

2.1 Materials and Preparation

A commercial PU coating containing 5 % mass fraction of nanosilica was used in this study. Two types of specimens were used. Specimens of free-standing films were used for UV degradation characterization and simulated rain-induced nanoparticle released study, while specimens of PU nanocoatings applied to wood substrate

[◇] Certain commercial product or equipment is described in this paper in order to specify adequately the experimental procedure. In no case does such identification imply recommendation or endorsement by the National Institute of Standards and Technology, nor does it imply that it is necessarily the best available for the purpose.

having a dimension of 2.35 cm x 2.08 cm were adopted for measuring nanoparticle release by abrasion after weathering. Details of sample compositions and preparation of the free-standing films were described in reference.⁸ Specimens of PU nanocoatings coated wood substrates were prepared using the same procedure by applying coatings via drawdown technique directly on wood substrates instead of on a polyethylene terephthalate (PET) sheet. Due to absorption by the wood substrate, two layers of coatings were needed to ensure a good coverage of coatings. All samples were conditioned at room temperature for three weeks before use.

2.2 UV Expoure

Specimens for weathering were exposed in the NIST SPHERE at 50 °C and approximately 0 % relative humidity (R.H.). The SPHERE,¹² an abbreviation of Simulated Photodegradation via High Energy Radiant Exposure, is a NIST-developed 2 m integrating sphere weathering chamber that provides high intensity, uniform UV radiation, with well-controlled environments. Specimens were removed after specified time intervals for various characterizations and/or post exposed experiments such as abrasion or rain simulation to induce particle release.

2.3 Surface Morphology Characterization

Surface morphology were characterized by LSCM and AFM. LSCM was performed using a Zeiss model LSM510 and a laser wavelength of 543 nm. LSCM were carried out using 50x (scan area 170 μm x 170 μm) and 150 x (56 μm x 56 μm) magnification. LSCM images presented here are two dimensional (2D) projections in the X-Y plane. AFM imaging was used Dimension Icon system (Bruker) and silicon probes (TESP, Bruker) at ambient conditions (24°C, 50 % RH). Resonance frequency of measuring was approximately 300 kHz.

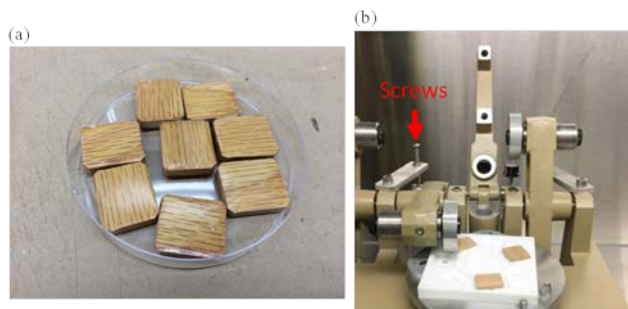


Figure 1. Picture of (a) nanocoatings coated wood specimens, and (b) abrasion setup using taber rotary abraser. The screw were used to adjust vertical postion of the wheel.

2.4 Abrasion

A Taber rotary abraser (Model 5155, Taber, North Tonawanda, NY) and a NIST-developed metallic wheel

(MW2) were used in this study. To adapt the small UV-exposed coated wood specimens (2.35 cm x 2.08 cm), as showed in Figure 1(a), a Teflon sample holder/adaptor (100 mm x 100 mm, which is the standard sample size for abrader) was fabricated, as displayed in Figure 1(b). This small size was used so that a large number of specimens can be simultaneously exposed in the NIST SPHERE. Each Teflon holder contained seven 2.35 cm x 2.08 cm openings located along the path of the abrasion wheel. Each individual specimen was securely fitted into each opening of the holder. Only three exposed specimens were used for each abrasion test. Therefore, to prevent the wheel from tumbling into the unoccupied openings, a set of screws (red arrow) was placed on the wheel's support arm to adjust the vertical position shown in Figure 1(b). The abrasion was conducted at a speed of 60 rpm (6.28 rad/s), 100 cycles, and a fixed load having a force closed to the mass of the wheel (178 g). Inductively coupled plasma-optical emission spectroscopy (ICP-OES) was used to quantify the mass of silicon (Si, assuming is from nanosilca particles) released from the materials collected from the abrasion wheel. ICP-OES analyses were performed using an Optima 5300 DV instrument (Perkin Elmer, Shelton, CT). Details of measurement and protocols were described in reference.⁸

3 RESULTS AND DISCUSSION

3.1 Surface Morphology after UV Exposure

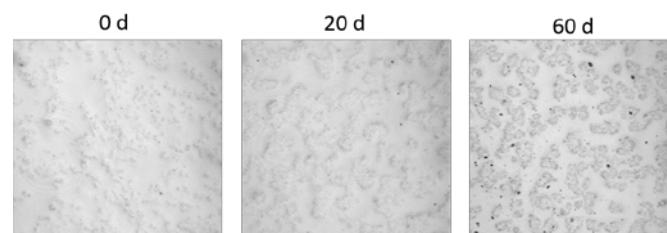


Figure 2. LSCM images at 50x magnifications of the nanocoating surface exposed at different exposure times (d for day). The image size is 170 μm x 170 μm.

Figure 2 displays the LSCM images (50x magnification) of surface morphology of nanocoating at three different exposure times. Before abrasion (0 d), the surface appeared to be rough with some under surface features. After 20 d under UV exposure, the surface features became more visible and surface roughness increased. The root-mean-square (rms) surface roughness values increased from $0.09 \mu\text{m} \pm 0.01 \mu\text{m}$ at 0 d to $0.15 \mu\text{m} \pm 0.07 \mu\text{m}$ at 20 d. The rms roughness values were the average obtained from 6 measurements and the uncertainty represented hereis one standard deviation. As expoure time increased, these surface morphological changes became more pronounced. At 60 d, the rms value is similar to that of 20 d, but many clusters-like features were visible on the coating surfaces.

To examine the surface morphological changes closely, AFM measurements were performed on the free-standing films (smoother surface) at different exposure times, as shown in Figure 3. Before exposure (0 d), there was featureless in phase image (right-hand-side column). Particle-like or cluster-like features appeared at 26 d, and the cluster size became larger at 64 d. Note that in phase imaging, the bright and dark domains generally correspond to hard and soft materials, respectively (silica has a modulus of 79 GPa and polymers have a modulus < 1 GPa). Thus the bright spots in phase image (indicated by arrows) for 26 d and 64 d are assuming to be nanosilica clusters, which are consistent with the observation in the height images. This result was confirmed through scanning electron microscopy with energy dispersive X-ray (SEM/EDX) results in our previous study.⁸

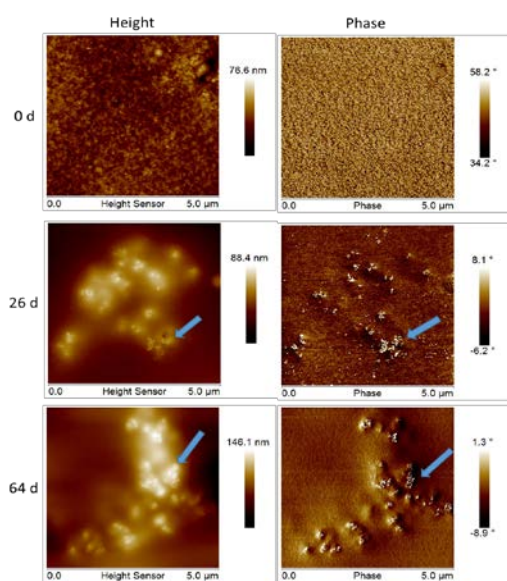


Figure 3. Representative AFM phase and height images (5 μm x 5 μm scan size) obtained at different exposure times (d for day), showing clearly individual nanoparticles and clusters (blue arrow) on nanocoating specimens' surface after exposed under UV for 26 d, 64 d. The ranging indicators for height and phase were also displayed next to images.

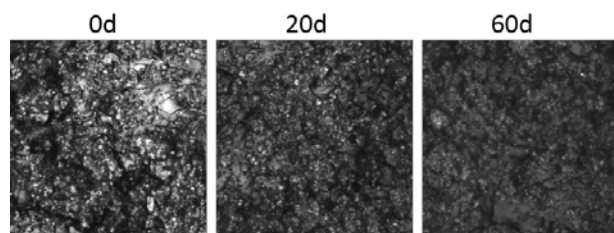


Figure 4. LSCM images at 150x magnifications of abraded nanocoating surfaces at different exposure days (d). The image size is 56 μm x 56 μm.

3.2 Surface Morphology after Abrasion

After exposed under UV for (0, 10, 20, 40, 60) d, nanocoatings were abraded using the same protocol at a speed of 60 rpm (6.28 rad/s), 100 cycles, and a fixed load. Figure 4 displays LSCM images at 150x magnifications of abraded surfaces at different exposure times. Note that we have also imaged different locations on the samples holder and confirmed that particles released by abrasion can be found only on the locations just after the wheel has passed in the direction of the wheel travel. Little evidence of any particles released by abrasion was observed outside the abraded specimen. Further, a substantial amount of released particles by abrasion of weathered nanocoatings were still attached to the wheel. The average mass lost after abrasion for different exposed times are given in Table 1. The mass loss values were measured as a direct subtraction of exposed specimen masses before and after abrasion for three samples.

3.3 Analyses of LSCM images

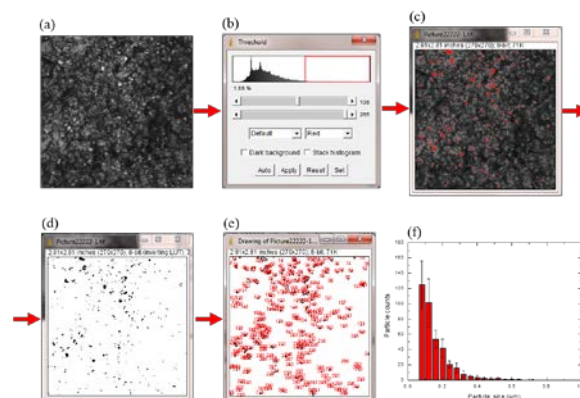


Figure 5. (a-e): Procedure for LSCM image analysis (f): Number and size distributions of particles released per 1 mm² abraded area of nanocoating after UV exposed

Image analysis was applied to LSCM image in order to quantify the number and distribution of particles on the abraded surface. Figure 5 illustrates an example of the process and result of this analysis for a 150x LSCM image obtained on coating surface after abrasion. A LSCM image of the abraded surface shows numerous bright dots in grey/dark grey background (Figure 5a). Brighter areas in an LSCM image represent regions that scatter more light than darker areas. Due to a higher index of reflection of metal-oxide or oxide particles, the bright dots observed are believed to be the particles, possibly containing silica particles. By selecting and fine tuning the grey level threshold (Figure 5b), bright dots in the images are highlighted (Figure 5c) and the number of particles (or their clusters) for each size are tallied from the occupied pixel area in a 2D LSCM projection image. The number and size distribution of particles present in this paper is from at least

8 LSCM images with a measurement area of $56 \mu\text{m} \times 56 \mu\text{m}$ ($3.14 \times 10^{-3} \text{mm}^2$) on coating surface (figure 5f).

3.4 Quantification of Released Particles on the Abraded Surfaces

Figure 6 (a-e) show particle number and size distribution obtained from LSCM images for different exposure times. The number of released particles decreased exponentially with increasing particle size for all exposure times, with the lowest particle size had the greatest number of released particles. Figure 6f shows the total number of released particles remained on the abraded nanocoating surface that had been exposed for 20 d or longer appeared to be greater than those abraded before 10 d exposed.

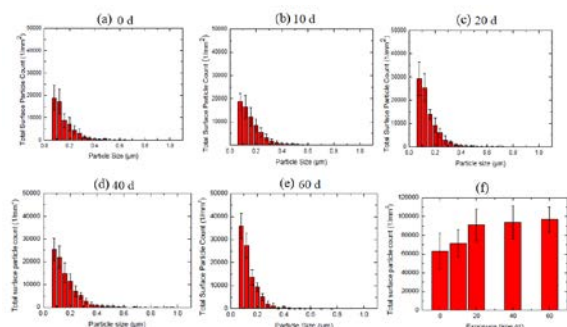


Figure 6. (a-e): Number and size distributions of particles released per 1mm^2 abraded area of nanocoating exposed for different times (f): Total number of particles released per 1mm^2 abraded area of nanocoating exposed for different times. All results are average of 8 measurements, and the error bars represent one standard deviation.

3.5 Quantification of Nanoparticles Released from the Abrader Wheels

To quantify the amounts of Si in the particles released by abrasion, samples collected from abrasion were analyzed by ICP-OES. As mentioned in section 3.2, substantial amount of released particles were obtained from the wheels. Therefore, the collection of released particles on the wheel was performed by thoroughly rinsing the wheel with water after abrasion. The amounts of Si detected using ICP-OES for different exposure times are listed in Table 1. An average of $2 \mu\text{g}$ of Si was detected after abrasion for each exposure time. It may be that most of silica nanoparticles are still embedded in the PU matrix when the nanoparticles are released by mechanical forces. In the previous simulated-rain induced particle release study,⁸ the amounts of released Si slowly increased with exposure times. The mass of Si was $1 \mu\text{g}$ around 14 d and remained constant, until the 87 d exposure time the released Si mass increased to $4 \mu\text{g}$. The ICP results obtained from the simulated rain method is different from that using abrasion method. The reason is stated as follows. The particles release via

abrasion method comes from the mechanical forces and particles release will be easy and the total particles attached on abrasion wheel at different exposure times are almost the same. The particles release via simulated rain method was layer by layer from water rinse; it increases with the exposure time, and is more than that of abrasion system.

Table 1. Mass loss before and after abrasion of exposed nanocoating on wood at different exposure time; Amount of Si released by abrasion after exposed nanocoating for different times. The results are average of six specimens and the numbers after the \pm symbol represent one standard deviation.

Exposure Time (d)	0	20	60
$M_{\text{before}} - M_{\text{after}}$ (mg)	0.15 ± 0.10	2.20 ± 0.27	1.98 ± 0.17
Mass of Si (μg) by ICP	2.2 ± 1.4	2.01 ± 0.51	1.92 ± 0.50

4 CONCLUSIONS

The mechanism and process of nanosilica release of a commercial polyurethane nanocoating were investigated through a combination of UV exposure and mechanical abrasion. The morphological changes, mass loss, and Si released of UV exposed-then-abraded samples were characterized by LSCM, AFM, and ICP-OES techniques. Based on the experimental results, the following conclusions can be obtained: Silica nanoparticles were observed to accumulate on the nanocoating surface, and the amount of silica nanoparticles increases with increasing the UV exposure time. After abrasion test, the mass loss of nanocoatings under 20 d UV exposure was larger than that of 0 d exposure. However, the difference in the mass loss of nanocoatings between 20 and 60 d exposure is small. The ICP-OES results showed that the amount of nanoparticle release (mass of Si) in both abrasion and simulated rain method system increases with exposure time. From the release mass of Si ($2 \mu\text{g}$ via abrasion vs $1 \mu\text{g}$ via simulated rain), it is reasonable to understand different release mechanism of these two methods.

REFERENCES

- Zou, H, Wu, SS, Shen, J, Chem. Rev., 108 3893-3957 (2008)
- S. Pavlidou and C. D. Papaspyrides, Prog. Polym. Sci, 33 1119-1198 (2008)
- A. J. Arosby, J. Y. Lee, Polymer Reviews, 47 217-229 (2007)
- F. Croce, G. Appetecchi, et al. Nature, 394 456-458 (1998)
- E.J. Petersen, et al. Environ Sci Technol. 49:9532-9547(2015)
- H. Godwin, C. Nameth, et al. ACS Nano. 9:3409-3417 (2015)
- W. Wohlleben, N. Neubauer, NanoImpact, 1 39-45 (2016)
- D. Jacobs, et al. , J. Coat. Technol. Res.,13(5) 735-751 (2016)
- W. Wohlleben, et al. , Environ. Chem. 11 (4) 402-418, (2014)
- H. C. Hsueh, et al. , Coat. Technol. Res., DOI 10.1007/s11998-016-9911-4 (2017)
- F. Gottschalk, J. Environ. Monit. 13 (5) 1145-1155 (2011)
- J. Chin, E. Byrd, et al., Rev. Sci. Instrum., 75 4951-4959 (2004)